Electronic Supplementary Information

Design and preparation of new luminescent metal-organic frameworks and different doped isomers: sensing pollution ions and enhancement of gas capture capacity

Dan Wu, Jianguo Cheng, Meng Wang, Jiao Liu, Jing Jin, Guoping Yang*, Wenyan Zhang and Yao-Yu Wang

Key Laboratory of Synthetic and Natural Functional Molecule of the Ministry of Education, Shaanxi Key Laboratory of Physico-Inorganic Chemistry, College of Chemistry & Materials Science, Northwest University, Xi'an, 710127, Shaanxi, P. R. China.

E-mail: ygp@nwu.edu.cn.

Section S1 Materials and general methods

All the reagents and solvents were purchased to use without further purification in the experiments. Elemental analyses (C, H, and N) were measured on Perkin-Elmer 2400C elemental analyser. Infrared spectra were examined on Bruker EQUINOX-55 spectrophotometer in 4000 − 400 cm^{-1} (KBr pellets). Powder X-ray diffraction patterns were investigated through Bruker D8 ADVANCE X-ray powder diffractometer. Thermogravimetric analyses were tested on NETZSCH STA 449C microanalyzer (N_2 atmosphere, 10 °C min^{-1}). Solid state luminescent spectra were determined via Hitachi F-4500 spectrophotometer at room temperature (RT). UV-vis spectra were measured on Hitachi U-3310 spectrometer. Inductively coupled plasma (ICP) analyses were carried out on IRIS Advantage spectrometer. Scanning electron microscopy (SEM) analyses were tested on SU8010 Field Emission Scanning Electron Microscope. X-ray photoelectron spectroscopy (XPS) measurements were performed on AXIS Ultra spectrometer. The gas sorption isotherms were tested on ASAP 2020 M sorption equipment.

Section S2 Crystallographic data collection and refinement

The single-crystal diffraction data were recorded on a Bruker SMART APEX II CCD detector by Mo-Kα radiation (λ = 0.71073 Å). The structures of MOFs were solved via the direct methods and refined through the full-matrix least-squares method based on F^2 on the SHELXL and Olex2 program.[1] All non-hydrogen atoms were refined anisotropically with the hydrogen atoms being calculated and assigned their ideal positions with isotropic displacement factors. The SQUEEZE of PLATON program was applied for **1** because of the disorder of the solvent molecules. The final formulae of **1** was determined by combination of the single-crystal structure, elemental analysis and TGA together.

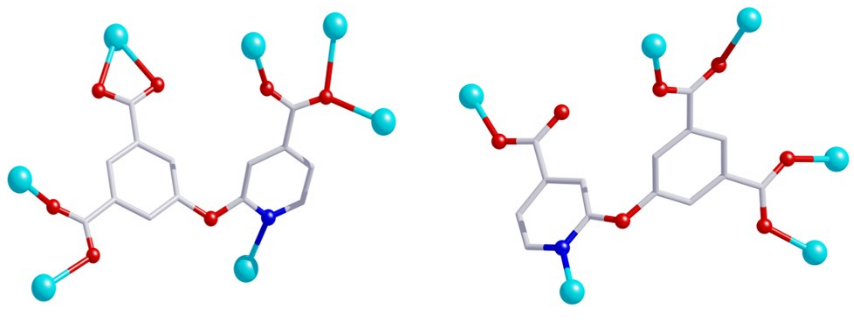

(a) **(b)**

Fig. S1 Coordination mode of L^{2-} in **1** (a) and **2** (b).

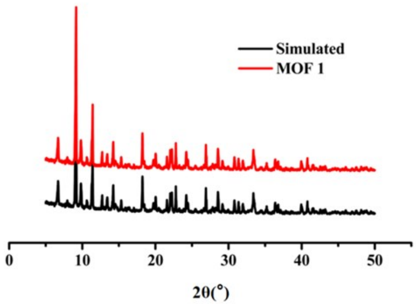

(a)

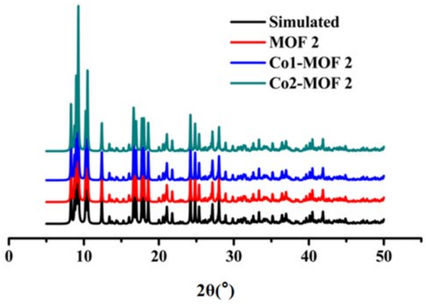

(b)

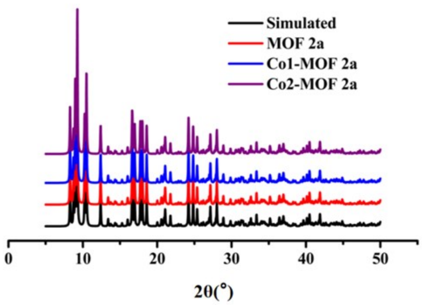

(c)

Fig. S2 PXRD patterns of the as-synthesized products and activated sample.

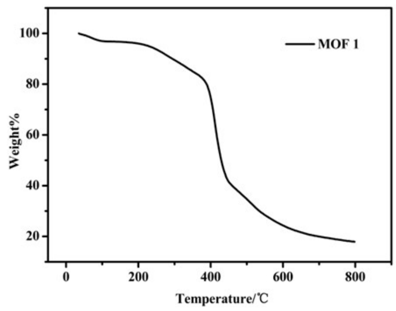

(a)

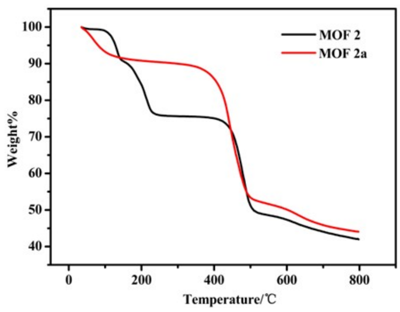

(b)

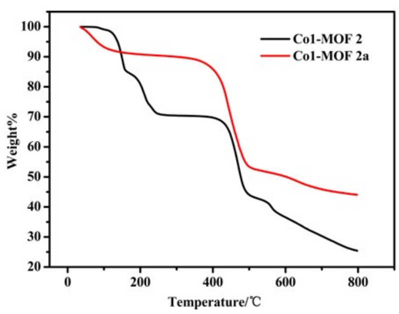

(c)

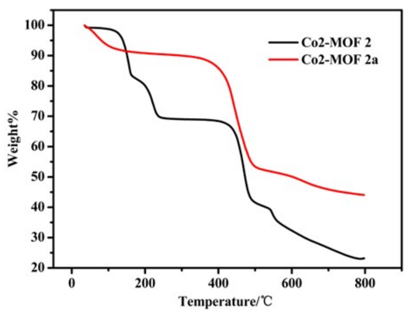

(d)

Fig. S3 TGA curves for the as-synthesized products and activated sample.

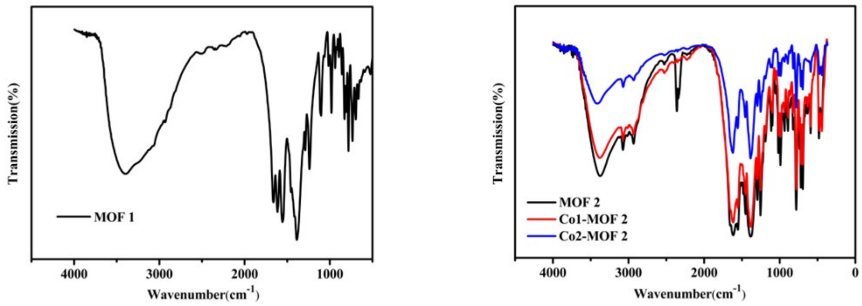

(a) **(b)**

Fig. S4 FT-IR spectra of the as-synthesized sample.

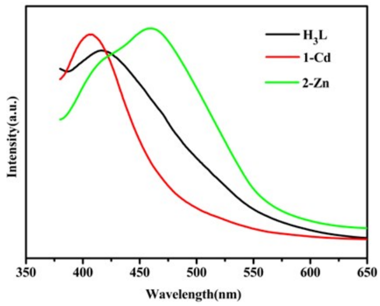

Fig. S5 Luminescent emission spectra of the free ligand H_3L and complexes **1-2** at room temperature.

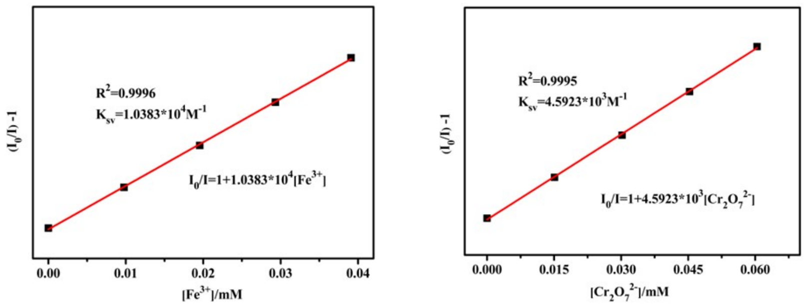

(a) **(b)**

Fig. S6 The linear correlation for the plot of (I_0/I) - 1 *vs.* concentration of Fe^{3+} (a) and $Cr_2O_7^{2-}$ (b) in low concentration range, respectively.

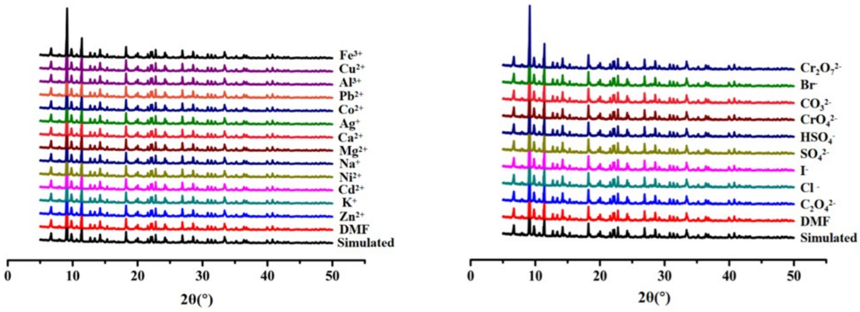

(a) **(b)**

Fig. S7 PXRD patterns of **1** treated by different $M(NO_3)_n$ solutions (a) and K_nA solutions (b).

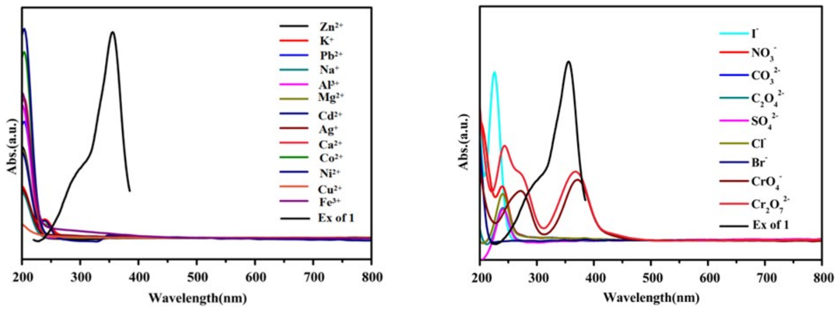

Fig. S8 (a) UV-vis adsorption spectrum of cations in DMF solution and the excitation spectrum of **1** in DMF solution; (b) UV-vis adsorption spectra of anions in DMF solution and the excitation spectrum of **1** in DMF solution.

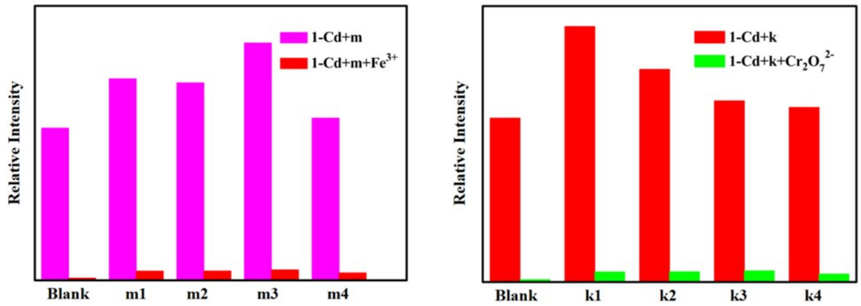

(a) **(b)**

Fig. S9 (a) Luminescence intensity of **1** dispersed in DMF with addition of different mixed metal ions (10^{-1}M) mixed solution added Fe^{3+} ions (10^{-1} M) (m1: Cu^{2+}/Al^{3+}/Na; m2: Zn^{2+}/Co^{2+}; m3: K^{+}/Mg^{2+}/$^{+}Cd^{2+}$; m4: Ca^{2+}/Ni^{2+}), and (b) with addition of different mixed anion ions (10^{-1} M) mixed solution added $Cr_2O_7^{2-}$ ions (10^{-1} M) (k1: Cl^-/Br^-/I^-; k2: IO_3^-/BrO_3^-; k3: $C_2O_4^{2-}$/CO_3^{2-}; k4: SO_4^{2-}/NO_3^-).

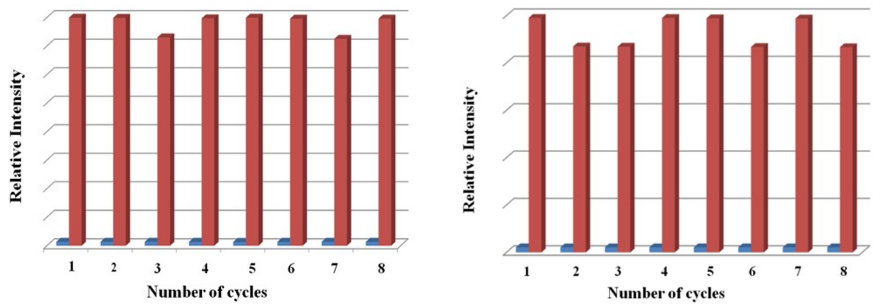

(a) **(b)**

Fig. S10 Multiple cycles for the fluorescence quenching of **1** by Fe^{3+} (a) and $Cr_2O_7^{2-}$ (b), and recovery after washing by DMF for several times.

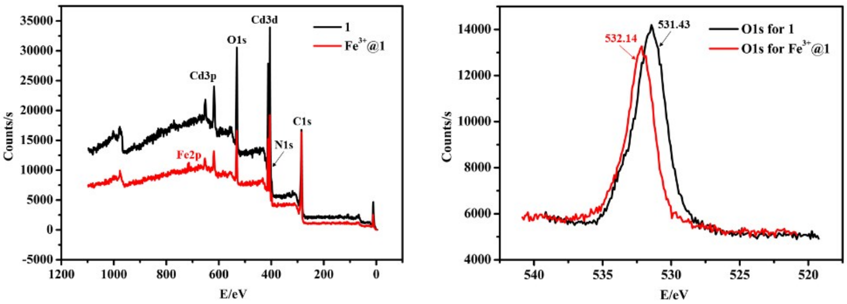

(a) (b)

Fig. S11 (a) XPS spectra of the **1** and Fe^{3+}@**1**; (b) O1s XPS spectra of the **1** and Fe^{3+}@**1**.

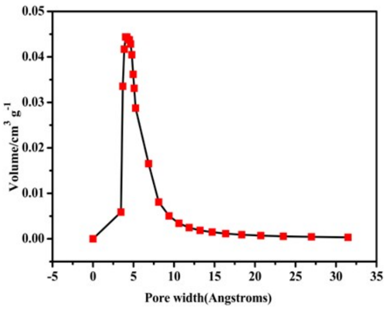

Fig. S12 Pore size distribution (inset) of **2**.

IAST adsorption selectivity calculation

The experimental isotherm data for pure CO_2 and CH_4 (measured at 273 and 298 K) were fitted using a Langmuir-Freundlich (L-F) model

$$q = \frac{a * b * p^c}{1 + b * p^c}$$

Where *q* and *p* are adsorbed amounts and pressures of component *i*, respectively. The adsorption selectivities for binary mixtures of CO_2/CH_4 at 273 and 298 K., defined by

$$S_{ads} = (\frac{q1}{q2}) / (\frac{p1}{p2})$$

Where *qi* is the amount of *i* adsorbed and *pi* is the partial pressure of *i* in the mixture.

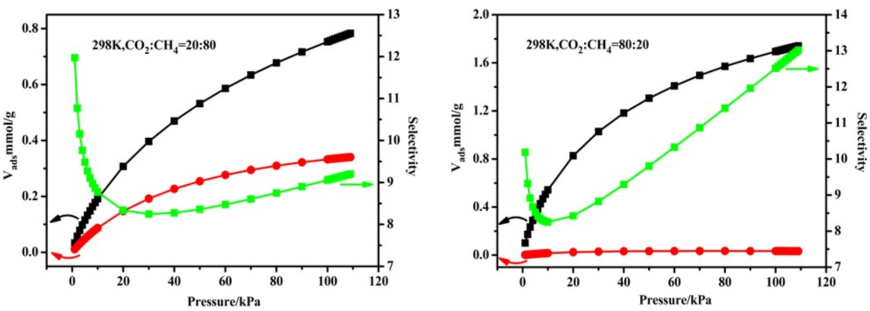

(a) (b)

Fig. S13 IAST adsorption selectivity of **2** for different ratios CO_2/CH_4 at 298 K.

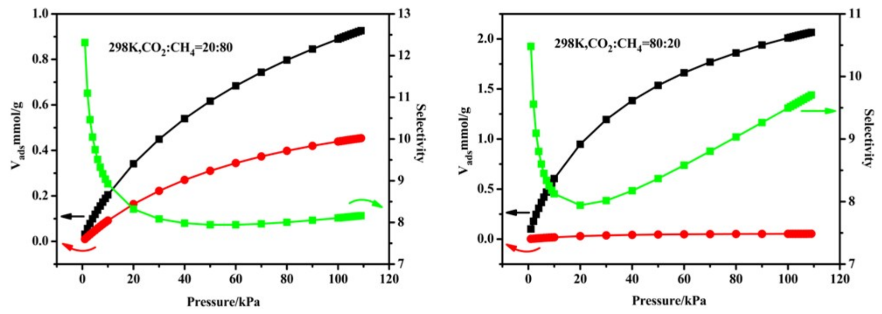

(a) **(b)**

Fig. S14 IAST adsorption selectivity of Co1-MOF **2** for different ratios CO_2/CH_4 at 298 K.

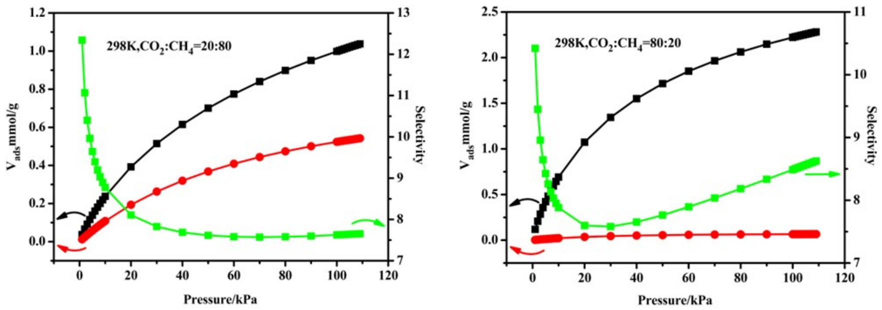

(a) **(b)**

Fig. S15 IAST adsorption selectivity of Co2-MOF **2** for different ratios CO_2/CH_4 at 298 K.

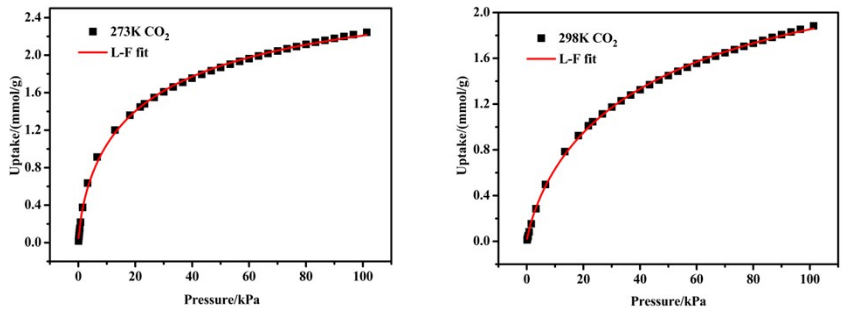

(a) **(b)**

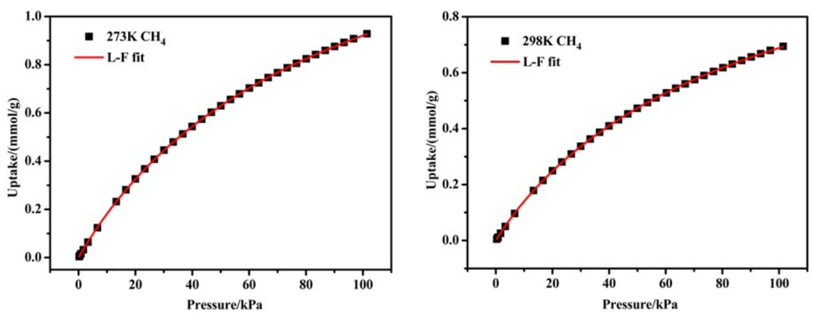

(c) **(d)**

Fig. S16 CO_2 (a) and CH_4 (c) adsorption isotherms of **2** at 273 K with fitting; CO_2 (b) and CH_4 (d) adsorption isotherms of **2** at 298 K with fitting by L-F model.

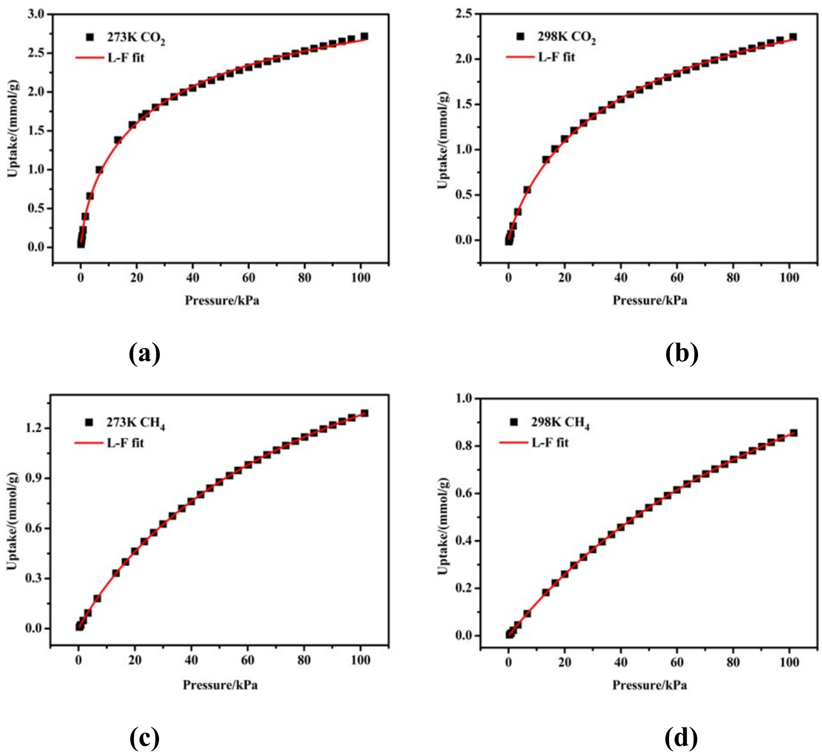

Fig. S17 CO_2 (a) and CH_4 (c) adsorption isotherms of Co1-MOF **2** at 273 K with fitting; CO_2 (b) and CH_4 (d) adsorption isotherms of Co1-MOF **2** at 298 K with fitting by L-F model.

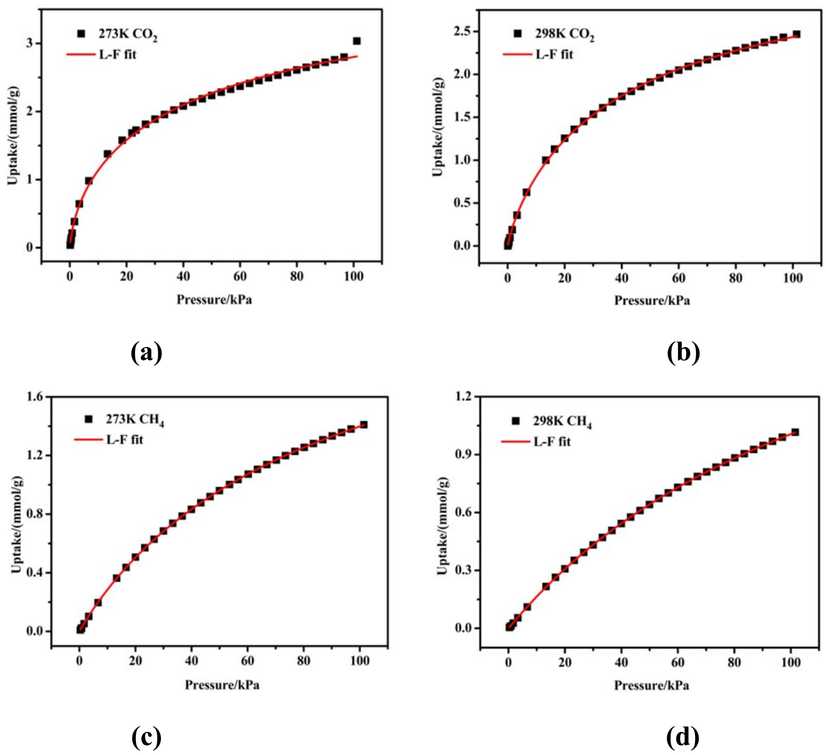

Fig. S18 CO_2 (a) and CH_4 (c) adsorption isotherms of Co2-MOF **2** at 273 K with fitting; CO_2 (b) and CH_4 (d) adsorption isotherms of Co2-MOF **2** at 298 K with fitting by L-F model.

Calculation of sorption heat for CO_2 and CH_4 uptake using Virial 2 model

The CO_2 and CH_4 adsorption isotherm data for **2** at 298 K were fitted using the Virial 2 expression, where P is the pressure, N is the adsorbed amount, T is the temperature, a_i and b_i are virial coefficients, and m and N are the number of coefficients used to describe the isotherms. Q_{st} is the coverage–dependent enthalpy of adsorption and R is the universal gas constant.

$$\ln P = \ln N + 1/T\sum_{i=0}^{m} a_i N^i + \sum_{i=0}^{n} b_i N^i \qquad Q_{st} = R\sum_{i=0}^{m} a_i N^i$$

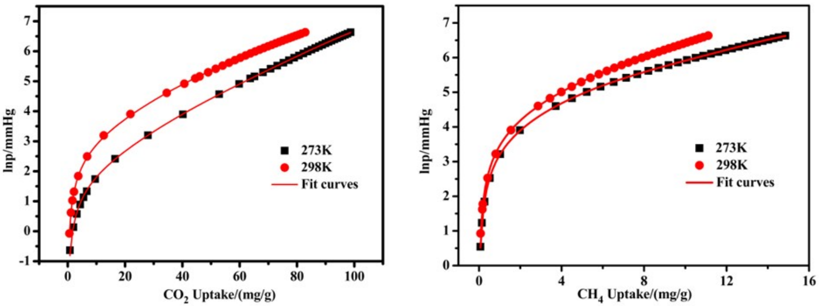

(a) (b)

Fig. S19 (a) CO_2 adsorption isotherms for **2** with fitting by Virial 2 model, fitting results: a0 = -3454.82324, a1 = -10.03395, a2 = 0.58418, a3 = -0.00699, a4 = 6.10908E-5, a5 = -2.0822E-7, b0 = 12.15463, b1 = 0.02454, b2 = -6.76085E-4, Chi^2 = 8.23796E-4, R^2 = 0.9998; (b) CH_4 adsorption isotherms for **2** with fitting by Virial 2 model, fitting results: a0 = -799.39442, a1 = -72.62152, a2 = 5.62545, a3 = -1.3822, a4 = 0.09116, a5 = -0.0022, b0 = 6.14821, b1 = 0.20517, b2 = 0.01468, Chi^2 = 1.64039E-4, R^2 = 0.99993.

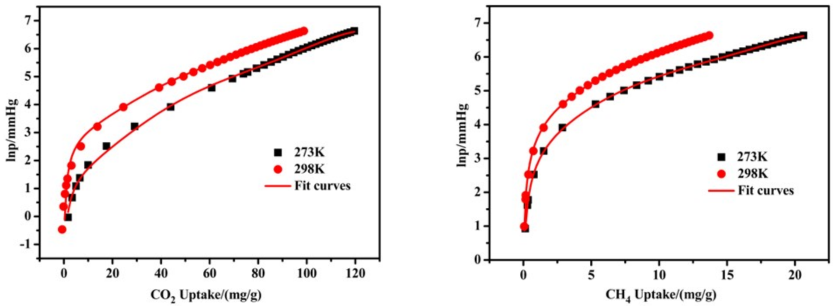

(a) (b)

Fig. S20 (a) CO_2 adsorption isotherms for Co1-MOF **2** with fitting by Virial 2 model, fitting results: a0 = -4699.88473, a1 = 39.18932, a2 = 0.58585, a3 = -0.01687, a4 = 1.33364E-4, a5 =-3.88988E-7, b0 = 16.93474, b1 = -0.20335, b2 =0.00134, Chi^2 = 0.01593, R^2 = 0.99592; (b) CH_4 adsorption isotherms for Co1-MOF **2** with fitting by Virial 2 model, fitting results: a0 =-2513.94782, a1 = 39.79797, a2 = 4.72359, a3 = -1.09827, a4 = 0.05294, a5 = -9.2996E-4, b0 = 12.09386, b1 = -0.25015, b2 =0.01978, Chi^2 = 6.62276E-4, R^2 = 0.99972.

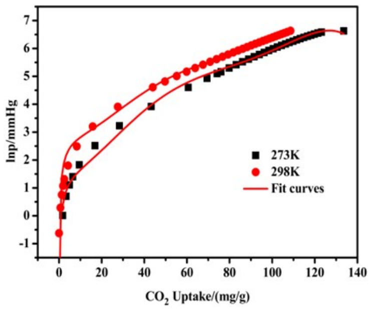

(a)

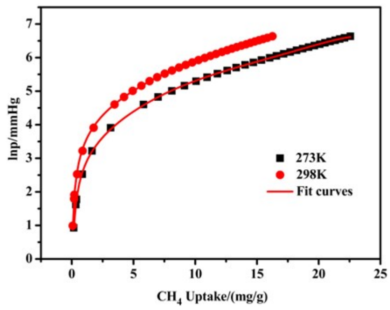

(b)

Fig. S21 (a) CO_2 adsorption isotherms for Co2-MOF **2** with fitting by Virial 2 model, fitting results: a0 = -4295.27252, a1 = 40.28878, a2 = 1.19539, a3 = -0.0291, a4 = 2.19645E-4, a5 = -6.06638E-7, b0 = 15.76567, b1 = -0.2685, b2 = 0.00179, Chi^2 = 0.18873, R^2 = 0.95208; (b) CH_4 adsorption isotherms for Co2-MOF **2** with fitting by Virial 2 model, fitting results: a0 = -2252.06704, a1 = 40.39341, a2 = 4.67411, a3 = -0.83984, a4 = 0.03671, a5 = -5.85339E-4, b0 = 11.04704, b1 = -0.24576, b2 = 0.01418, Chi^2 = 6.31418E-4, R^2 = 0.99973.

Table S1 Selected bond lengths [Å] and angles [º] for **1-2**

Complex 1			
Cd(1)-O(4)#1	2.396(6)	N(1)#4-Cd(1)-O(4)#1	112.8(2)
Cd(1)-O(6)#2	2.303(4)	N(1)#4-Cd(1)-O(7)#3	144.00(18)
Cd(1)-O(3)#1	2.283(7)	O(2)-Cd(2)-O(2)#5	152.1(3)
Cd(1)-O(7)#3	2.415(5)	O(2)-Cd(2)-O(7)#3	83.55(18)
Cd(1)-O(1)	2.231(5)	O(2)-Cd(2)-O(7)#2	118.87(19)
Cd(1)-N(1)#4	2.367(5)	O(2)#5-Cd(2)-O(7)#3	118.87(19)
Cd(2)-O(2	2.265(5)	O(2)#5-Cd(2)-O(7)#2	83.56(18)
Cd(2)-O(2)#5	2.265(5)	O(2)#5-Cd(2)-O(8)#5	81.0(8)
Cd(2)-O(7)#3	2.336(5)	O(2)-Cd(2)-O(8)#5	84.4(6)
Cd(2)-O(7)#2	2.336(5)	O(2)#5-Cd(2)-O(8)	84.4(6)
Cd(2)-O(8)	2.366(16)	O(2)-Cd(2)-O(8)	81.0(8)
Cd(2)-O(8)#5	2.366(16)	O(2)-Cd(2)-O(8A)	95.2(8)
Cd(2)-O(8A)#5	2.355(15)	O(2)#5-Cd(2)-O(8A)#5	95.2(8)
Cd(2)-O(8A)	2.355(15)	O(2)#5-Cd(2)-O(8A)	75.9(6)
O(4)#1-Cd(1)-O(7)#3	99.63(19)	O(2)-Cd(2)-O(8A)#5	75.9(6)
O(6)#2-Cd(1)-O(4)#1	144.2(2)	O(7)#3-Cd(2)-O(7)#2	79.5(3)
O(6)#2-Cd(1)-O(7)#3	83.34(16)	O(7)#2-Cd(2)-O(8)	153.0(9)
O(6)#2-Cd(1)-N(1)#4	79.45(16)	O(7)#3-Cd(2)-O(8)	85.3(7)
O(3)#1-Cd(1)-O(4)#1	55.6(2)	O(7)#3-Cd(2)-O(8)#5	153.0(9)
O(3)#1-Cd(1)-O(6)#2	88.7(2)	O(7)#2-Cd(2)-O(8)#5	85.3(7)
O(3)#1-Cd(1)-O(7)#3	100.7(2)	O(7)#3-Cd(2)-O(8A)#5	135.7(10)
O(3)#1-Cd(1)-N(1)#4	110.3(3)	O(7)#3-Cd(2)-O(8A)	76.9(6)
O(1)-Cd(1)-O(4)#1	86.6(2)	O(7)#2-Cd(2)-O(8A)#5	76.9(6)
O(1)-Cd(1)-O(6)#2	128.8(2)	O(7)#2-Cd(2)-O(8A)	135.7(10)
O(1)-Cd(1)-O(3)#1	142.1(2)	O(8)#5-Cd(2)-O(8)	116.6(15)
O(1)-Cd(1)-O(7)#3	81.4(2)	O(8A)#5-Cd(2)-O(8A)	143.0(16)
O(1)-Cd(1)-N(1)#4	85.1(2)		

Symmetry transformations used to generate equivalent atoms: #1 x, y, z-1; #2 x+1/4, -y+5/4, z-3/4; #3 -x+5/4, y+1/4, z-3/4; #4 -x+3/2, -y+1, z-1/2; #5 -x+3/2, -y+3/2, z; #6 x, y, z+1; #7 x-1/4, -y+5/4, z+3/4; #8 -x+5/4, y-1/4, z+3/4; #9 -x+3/2, -y+1, z+1/2.

Complex 2			
Zn(1)-O(2)	2.0318(19)	O(12)#3-Zn(1)-O(7)#1	169.37(7)
Zn(1)-O(7)#1	2.1138(17)	O(12)#1-Zn(1)-O(7)#1	91.22(7)
Zn(1)-O(8)#2	2.0524(18)	O(12)#1-Zn(1)-O(12)#3	79.83(7)
Zn(1)-O(12)#3	2.1037(17)	O(12)#3-Zn(1)-O(13)	86.20(7)
Zn(1)-O(12)#1	2.0856(18)	O(12)#1-Zn(1)-O(13)	82.15(7)
Zn(1)-O(13)	2.2710(19)	O(13)-Zn(1)-Zn(2)#1	50.63(5)
Zn(2)-O(5)	1.9502(18)	O(5)-Zn(2)-Zn(1)#1	81.80(5)
Zn(2)-O(9)#4	1.9533(18)	O(5)-Zn(2)-O(9)#4	129.95(8)

Zn(2)-O(12)	1.9468(17)	O(5)-Zn(2)-O(13)#1	80.99(7)
Zn(2)-O(13)#1	2.4320(19)	O(5)-Zn(2)-N(1)#5	98.44(8)
Zn(2)-N(1)#5	2.109(2)	O(9)#4-Zn(2)-Zn(1)#1	118.06(6)
O(2)-Zn(1)-Zn(2)#1	134.39(5)	O(9)#4-Zn(2)-O(13)#1	83.20(8)
O(2)-Zn(1)-O(7)#1	92.61(8)	O(9)#4-Zn(2)-N(1)#5	92.71(9)
O(2)-Zn(1)-O(8)#2	91.30(8)	O(12)-Zn(2)-Zn(1)#1	40.87(5)
O(2)-Zn(1)-O(12)#3	95.10(7)	O(12)-Zn(2)-O(5)	109.95(7)
O(2)-Zn(1)-O(12)#1	168.34(7)	O(12)-Zn(2)-O(9)#4	113.91(7)
O(2)-Zn(1)-O(13)	87.06(7)	O(12)-Zn(2)-O(13)#1	80.94(7)
O(7)#1-Zn(1)-Zn(2)#1	71.67(5)	O(12)-Zn(2)-N(1)#5	104.80(8)
O(7)#1-Zn(1)-O(13)	86.91(7)	O(13)#1-Zn(2)-Zn(1)#1	46.21(4)
O(8)#2-Zn(1)-Zn(2)#1	129.50(6)	N(1)#5-Zn(2)-Zn(1)#1	139.74(6)
O(8)#2-Zn(1)-O(7)#1	89.12(7)	N(1)#5-Zn(2)-O(13)#1	173.98(7)
O(8)#2-Zn(1)-O(12)#1	99.77(7)	Zn(1)#1-O(12)-Zn(1)#8	100.17(7)
O(8)#2-Zn(1)-O(12)#3	97.98(7)	Zn(2)-O(12)-Zn(1)#8	113.84(8)
O(8)#2-Zn(1)-O(13)	175.63(7)	Zn(2)-O(12)-Zn(1)#1	101.48(8)
O(12)#1-Zn(1)-Zn(2)#1	37.65(5)	Zn(1)-O(13)-Zn(2)#1	83.16(6)
O(12)#3-Zn(1)-Zn(2)#1	97.70(5)		

Symmetry transformations used to generate equivalent atoms: #1 -x+2, -y+2, -z+1; #2 x, y, z-1; #3 x-1, y, z-1; #4 x+1, y, z; #5 -x+2, -y+1, -z+1; #6 x, y, z+1; #7 x-1, y, z; #8 x+1, y, z+1.

Table S2 ICP analyses for **2**, Co1-MOF **2** and Co2-MOF **2**

Compound	Concentration of Zn(II) (ppb)	Concentration of Co(II) (ppb)	Zn/Co(II)
2	17533.41	0	-
Co1-MOF **2**	18137.48	7750.32	2.34
Co2-MOF **2**	10469.28	15543.49	0.67

Table S3 Adsorption selectivity of reported MOFs for CO_2/CH_4 (50:50) at 1 bar

Compound	Adsorption selectivity of CO_2/CH_4	Temperature/ K	Ref.
SIFSIX-2-Cu	5.3	298	2
JUC-141	8.72	298	3
Zeolite 13X	3.6	298	4
Activated carbon	2.3	298	4
UiO-66	6.87	298	5
JUC-199	9.0	298	6
Complex-**1**	12.3	298	7
Complex-**2**	10.73	298	**This work**
Co1-MOF **2**	8.77	298	**This work**
Co1-MOF **2**	8.02	298	**This work**

Table S4 Equation parameters for the DSLF isotherm model for **2**, Co1-MOF **2**, Co2-MOF **2**

	a	B	c	Chi^2	R^2
2-273CO_2	3.03479	0.1032	0.0707	5.76004E-4	0.99905
Co1-MOF 2-273CO_2	3.83781	0.08349	0.71658	8.86384E-4	0.99885
Co2-MOF 2-273CO_2	4.60083	0.06932	0.67556	0.00296	0.9965
2-298CO_2	2.87709	0.04385	0.80801	2.1275E-4	0.99946
Co1-MOF 2-298CO_2	3.37003	0.03755	0.85166	4.864141E-4	0.99921
Co2-MOF 2-298CO_2	3.66114	0.04052	0.84547	2.36352E-4	0.99968
2-273CH_4	1.75188	0.01207	0.98141	1.05353E-6	0.99999
Co1-MOF 2-273CH_4	2.45437	0.01294	0.96226	4.02974E-6	0.99998
Co2-MOF 2-273CH_4	2.68445	0.01343	0.95443	4.8198E-6	0.99998
2-298CH_4	1.32158	0.01294	0.96226	1.1682E-6	0.99998
Co1-MOF 2-298CH_4	1.93918	0.00762	1.00399	1.28677E-6	0.99998
Co2-MOF 2-298CH_4	2.30279	0.00849	1.13474	1.84187E-6	0.99998

References

1. G. M. Sheldrick, SHELXL-2014, Program for Crystal Structure Refinement, University of Göttingen, Germany, 2014.
2. P. Nugent, Y. Belmabkhout, S. D. Burd, A. J. Cairns, R. Luebke, K. Forrest, T. Pham, S. Ma, B. Space, L. Wojtas, M. Eddaoudi and M. J. Zaworotko, Porous materials with optimal adsorption thermodynamics and kinetics for CO_2 separation, *Nature*, 2013, **495**, 80-84.
3. N. Zhao, F. Sun, P. Li, X. Mu and G. Zhu, An Amino-Coordinated Metal Organic Framework for Selective Gas Adsorption, *Inorg. Chem.*, 2017, **56**, 6938-6942.
4. Z. H. Rada, H. R. Abid, J. Shang, Y. He, P. Webley, S. Liu, H. Sun and S. Wang, Effects of amino functionality on uptake of CO_2, CH_4 and selectivity of CO_2/CH_4 on titanium based MOFs, *Fuel*, 2015, **160**, 318-327.
5. D. H. Hong and M. P. Suh, Enhancing CO_2 Separation Ability of a Metal Organic Framework

by Post Synthetic Ligand Exchange with Flexible Aliphatic Carboxylates, *Chem. - Eur. J.*, 2014, **20**, 426-434.

6. H. He, F. Sun, B. Aguila, J. A. Perman, S. Ma and G. Zhu, A bifunctional metal organic framework featuring the combination of open metal sites and Lewis basic sites for selective gas adsorption and heterogeneous cascade catalysis, *J. Mater. Chem. A*, 2016, **4**, 15240-15246.
7. X.-Y. Li, L.-N. Ma, Y. Liu, L. Hou, Y.-Y. Wang and Z. Zhu, Honeycomb Metal-Organic Framework with Lewis Acidic and Basic Bifunctional Sites: Selective Adsorption and CO2 Catalytic Fixation, *ACS Appl. Mater. Interfaces*, 2018, **10**, 10965–10973.